Cytotherapy, 2013; 15: 792–804

International Society for Cellular Therapy
ISCT®

Combined treatment with platelet-rich plasma and brain-derived neurotrophic factor-overexpressing bone marrow stromal cells supports axonal remyelination in a rat spinal cord hemi-section model

TENGFEI ZHAO[1,*], WEIQI YAN[2,*], KAN XU[2], YIYING QI[2], XUESONG DAI[1,2] & ZHONGLI SHI[2]

[1]*The Second Affiliated Hospital (Binjiang Branch) Zhejiang University School of Medicine, Hangzhou Binjiang Hospital, Hangzhou, China, and* [2]*Department of Orthopedic Surgery, 2nd Affiliated Hospital, Zhejiang University School of Medicine, Hangzhou, China*

Abstract

Background aims. Combining biologic matrices is becoming a better choice to advance stem cell-based therapies. Platelet-rich plasma (PRP) is a biologic product of concentrated platelets and has been used to promote regeneration of peripheral nerves after injury. We examined whether PRP could induce rat bone marrow stromal cells (BMSCs) differentiation *in vitro* and whether a combination of BMSCs, PRP and brain-derived neurotrophic factor (BDNF) could provide additive therapeutic benefits *in vivo* after spinal cord injury (SCI). *Methods.* BMSCs and BDNF-secreting BMSCs (BDNF-BMSCs) were cultured with PRP for 7 days and 21 days, respectively, and neurofilament (NF)-200, glial fibrillary acidic protein (GFAP), microtubule-associated protein 2 (MAP2) and ribosomal protein S6 kinase (p70S6K) gene levels were assessed. After T10 hemi-section in 102 rats, 15-μL scaffolds (PRP alone, BMSCs, PRP/BMSCs, BDNF-BMSCs or PRP/BDNF-BMSCs) were transplanted into the lesion area, and real-time polymerase chain reaction, Western blot, immunohistochemistry and ultrastructural studies were performed. *Results.* The messenger RNA expression of NF-200, GFAP, MAP2 and p70S6K was promoted in BMSCs and BDNF-BMSCs after culture with PRP *in vitro*. BDNF levels were significantly higher in the injured spinal cord after implantation of BDNF-BMSCs. In the PRP/BDNF-BMSCs group at 8 weeks postoperatively, more GFAP was observed, with less accumulation of astrocytes at the graft-host interface. Rats that received PRP and BDNF-BMSC implants showed enhanced hind limb locomotor performance at 8 weeks postoperatively compared with control animals, with more axonal remyelination. *Conclusions.* A combined treatment comprising PRP and BDNF-overexpressing BMSCs produced beneficial effects in rats with regard to functional recovery after SCI through enhancing migration of astrocytes into the transplants and axonal remyelination.

Key Words: *astrocyte migration, BDNF-overexpressing bone marrow stromal cells, platelet-rich plasma, remyelination, spinal cord injury*

Introduction

Spinal cord injury (SCI) can lead to devastating loss of neurologic function, affecting all levels below the site of injury. Injured axons in the mammalian spinal cord fail to regenerate across the lesion site and do not re-establish synaptic contacts with their destinations (1), largely because of a "natural barrier" and a diminished intrinsic regenerative capacity (2). This barrier consists of a cystic cavity and a non-permissive environment, which includes inhibitory extracellular matrices (3). As a consequence, severe trauma to the spinal cord usually results in long-lasting deficits, involving partial or complete paralysis and loss of feeling. Developing new strategies to treat such SCI is still a major clinical challenge (4).

Transplanting embryonic stem cells, neural stem cells and bone marrow stromal cells (BMSCs) are experimental treatments that have provided promising results for regenerating injured tissue and for improving neurologic function in animal models of SCI. Previous studies have reported that delivery of neurotrophic factors using different genetically engineered cells encourages axonal regeneration in the injured spinal cord (5,6). Compared with other

*These authors contributed equally to this work.

Correspondence: Dr **Xuesong Dai**, Department of Orthopedic Surgery, 2nd Affiliated Hospital, Zhejiang University School of Medicine, Hangzhou 310009, China. E-mail: daixshz@163.com; and Dr **Kan Xu**, Department of Orthopedic Surgery, The Second Affiliated Hospital, School of Medicine, Zhejiang University, Hangzhou 310009, China. E-mail: xukan@medmail.com.cn

(Received 19 July 2012; accepted 7 April 2013)

ISSN 1465-3249
http://dx.doi.org/10.1016/j.jcyt.2013.04.004

stem cells, BMSCs are easy to obtain, receptive to foreign gene transfer and exist in abundance (7,8). BMSCs are ideal cellular targets for genetic engineering and neurotrophic factor production. Because most of these cells die after transplantation as a result of ischemia and hypoxia followed by infiltration of inflammatory cells into the lesion zone, combined therapy using stem cells and biologic scaffolds is necessary to promote adhesion and differentiation of grafted cells. In addition, the cavity, surrounded with glia scar and other inhibitory extracellular matrices, may interfere with the re-growth of axon. The ideal biologic scaffold is important to minimize the physical gap, decrease formation of inhibitory extracellular matrices and reduce the inflammatory response. Platelet-rich plasma (PRP) is a biologic product of concentrated platelets that is collected from autologous blood. PRP secretes a large quantity of growth factors, including platelet-derived growth factor, transforming growth factor-β1 and transforming growth factor-β2, insulin-like growth factor-I and insulin-like growth factor-II, epidermal growth factor and vascular endothelial growth factor (9). Platelet-derived growth factor protects neurons by suppressing *N*-methyl-D-aspartic acid-evoked current and translocating the glutamate transporter to the cell membrane (10). Transforming growth factor-β1 increases synthesis of extracellular matrix components and promotes neuron survival (11). Insulin-like growth factor-I specifically enhances outgrowth of corticospinal motor neurons axons *in vitro* (12). PRP has been used to promote regeneration of peripheral nerves after injury, including the sciatic, cavernous and facial nerves (13–15). Previous studies have shown that the combined use of PRP and BMSCs has a synergistic effect on enhancing peripheral nerve regeneration (16). We reasoned that a PRP scaffold would potentiate the efficacy of BMSC-based treatments for SCI because most studies suggest that the cytokine receptors associated with PRP growth factors are widely localized on the surface of neurons and glia in the central nervous system (17). However, PRP contains few typical neurotrophic factors, such as BDNF, which play an early anti-inflammatory role and have been shown to promote sprouting of corticospinal tract neurons after SCI (18–20). Zurita *et al.* (21) demonstrated that PRP scaffolds with BDNF allowed most BMSCs to survive and differentiate into neural phenotype cells compared with fibrin scaffolds. We hypothesized that a combined treatment with BDNF-overexpressing BMSCs and a PRP scaffold in animals with SCI would have more beneficial effects for protecting neurons and promoting axonal regeneration.

Methods

Adenoviral vectors

Adenoviral replication-defective recombinant vectors (Microbix Biosystems, Mississauga, Ontario, Canada) are type 5 vectors that express transgenes under the transcriptional control of the cytomegalovirus promoter. Briefly, we amplified the coding sequence of rat BDNF complementary DNA (cDNA) by the reverse transcriptase polymerase chain reaction (PCR) and ligated them into the pDC315-EGFP plasmid (Genechem Co, Ltd, Shanghai, China) to produce pDC315-BDNF-EGFP. The identity of the BDNF cDNA obtained was confirmed by sequencing and comparison with the GeneBank sequence NM_012513.3. The rat BDNF primer sequence was forward, 5′-GAGGATCCCCGGGTACCGGTCG-CCACCATGACCATCCTTTTCCTTAC-3′, and reverse, 5′-TCACCATGGTGGCGACCGGTCTT-CCCCTTTTAATGGTC-3′. The pDC315-EGFP vector was propagated in HEK293 cells, purified and titered by endpoint dilution (titer = 1×10^9 plaque-forming units/mL).

BMSCs isolation, culture and adenovirus infection

BMSCs were purified as described previously (8,22). Briefly, BMSCs were harvested from tibias and femurs of 4-week-old Sprague-Dawley rats under aseptic conditions and purified and expanded in culture. Cells were maintained at 37°C in a humidified atmosphere with 5% carbon dioxide, and the medium was changed every 2 days. When adherent cells reached 80–90% confluence, they were detached with 0.25% trypsin-EDTA (Gibco, Shanghai, China) and re-plated at 1:3 in regular growth medium to allow for continued passaging. BMSCs of passage 3 with the same cell line were collected for either *in vitro* experiments or seeding into the scaffold. Cells performed a maximum of six doublings during expansion and culturing procedures. Monolayer cultured cells were detached by mechanical scratch and filtered through a stainless steel mesh filter to eliminate cell aggregates from the single-cell suspension. After centrifugation, cells were blocked with 1% bovine serum albumin for 15 min. Cells were then incubated with 5 μL of anti-mouse antibodies for 30 min on ice from Biolegend (San Diego, CA, USA): APC-CD44, APC/Cy7-CD45, PE/Cy7-CD73, Percp/Cy5.5-CD90 and FITC-CD105. Appropriate isotype control antibodies were used to exclude non-specific binding. After washing, the samples were analyzed using a BD FACSCanto II (BD Biosciences, San Jose, California, USA).

BMSCs were exposed to adenovirus-BDNF-GFP in 7 mL α-MEM medium for 12 h, with a multiplicity

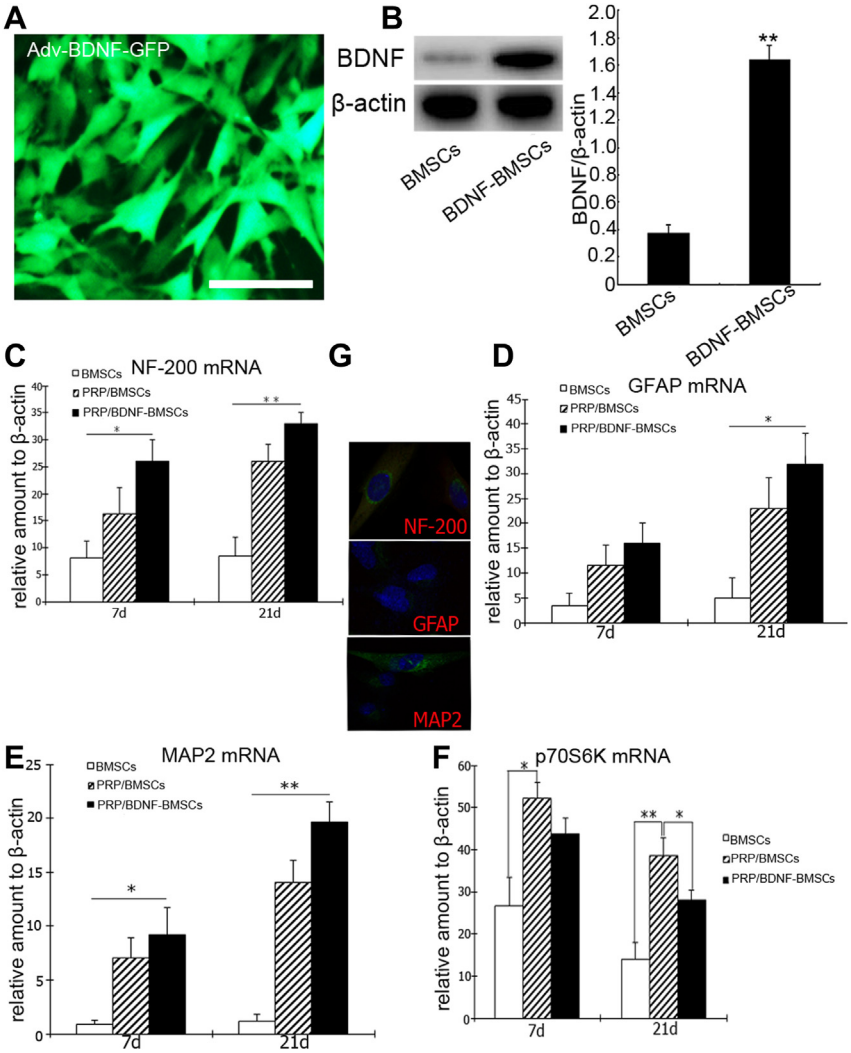

Figure 1. Expression of BDNF in BDNF-modified rat BMSCs and gene expression changes in BMSCs and BDNF-BMSCs combined with PRP *in vitro*. (A) BDNF expression in BMSCs after transfection with adenovirus-BDNF-GFP. (B) Western blot showing BDNF amounts in BMSCs after transfection with adenovirus-BDNF-GFP. (C–F) Gene expression changes after PRP culture for 7 days and 21 days. NF-200 (C), GFAP (D), MAP2 (E), p70S6K (F). Expression of NF-200, GFAP, MAP2 and p70S6K genes was promoted in BMSCs and BDNF-BMSCs after PRP culture *in vitro*. $^{*}P < 0.05$, $^{**}P < 0.01$. (G) Expression of NF-200, GFAP and MAP2 in PRP/BDNF-BMSCs group at 21 days after culturing with PRP was detected by immunofluorescence. Green represents GFP expression, which was associated with BDNF expression; the co-expression of BDNF with NF-200, GFAP or MAP2 (red) is not obvious in the PRP/BDNF-BMSCs group.

of infection of 100. The medium was removed, and the cells were washed once with α-MEM and re-cultured with normal medium. BDNF-secreting BMSCs (BDNF-BMSCs) were analyzed by flow cytometry. Rat BDNF enzyme-linked immunosorbent assay kits (Boster, Hubei, China) were used to quantify the BDNF concentration in the supernatant of BDNF-BMSCs or BMSCs. The implanted BMSCs were stained with chloromethyl-benzamido-dialkylcarbocyanine (CM-DiI; Molecular Probes, Carlsbad, California, USA) (23). Briefly, cells in suspension were washed with phosphate-buffered saline (PBS) and incubated with CM-DiI at a concentration of 2 μg/mL PBS for 5 min at 37°C and 15 min at 4°C. After labeling, CM-DiI-labeled BMSCs were washed several times with culture medium and applied to *in vivo* assay.

Preparation of PRP and BMSCs or BDNF-BMSCs loaded scaffolds

There were 27 Sprague-Dawley rats sacrificed to serve as a source of blood. From the right atrium of each rat, 4 mL of fresh blood treated with 3.8% sodium citrate was obtained in a sterile tube. Briefly, the platelets were enriched by a two-step centrifugation process, as described previously (22). PRP and whole blood samples were analyzed in an automatic counter (Model Sysmex F-820; Sysmex Co Ltd, Kobe, Japan). The average platelet concentration

Table I. Experimental groups and number of animals used for each examination.

Examinations		PRP groups			Control groups		
		PRP	PRP/BMSCs	PRP/BDNF-BMSCs	Vehicle	BMSCs	BDNF-BMSCs
PCR, Western blot (GFAP)	4w	3	3	3	0	3	3
	8w	3	3	3	0	3	3
IH+TEM	8w	8	8	8	8	8	8
Tracking cells	1w	0	3	0	0	3	0
	8w	0	3	0	0	3	0
Western blot (BDNF)	1w	0	3	3	0	3	3
Total		14	23	17	8	23	17

PRP, PRP group (scaffold only was prepared by 10 μL PRP, thrombin and calcium chloride with a total volume of 15 μL); PRP/BMSCs, PRP/BMSCs group (scaffold was prepared by 10 μL PRP, 3×10^5 BMSCs, thrombin and calcium chloride with a total volume of 15 μL); PRP/BDNF-BMSCs, PRP/BDNF-BMSCs group (scaffold was prepared by 10 μL PRP, 3×10^5 BDNF-BMSCs, thrombin and calcium chloride with a total volume of 15 μL); Vehicle, vehicle-treated group; BMSCs, BMSCs group, 15 μL of BMSC suspension (3×10^5 cells) was implanted; BDNF-BMSCs, BDNF-BMSCs group, 15 μL of BDNF-BMSCs suspension (3×10^5 cells) was implanted; PCR, quantitative reverse transcriptase polymerase chain reaction; Western blot (GFAP), Western blot for detecting GFAP expression *in vivo* at 8 weeks after surgery; IH, immunohistochemistry; TEM, transmission electron microscopy; Western blot (BDNF), Western blot for detecting BDNF expression *in vivo* at 1 week after surgery.

in whole blood was $2.06 \pm 0.46 \times 10^5$/μL before processing and reached $11.65 \pm 1.21 \times 10^5$/μL in the final PRP for transplantation. The specific growth factors in the PRP were not quantified in this study.

A 10-μL aliquot of PRP was polymerized with the cells that had mixed with thrombin (100 IU; Sigma-Aldrich, St Louis, Missouri, USA) containing calcium chloride (34 μmol/mL) as described previously (21), and a total of 3×10^5 cells/15 μL/explant was used. The BMSCs and BDNF-transduced BMSCs were also seeded onto 25-mL flasks at a density of 3×10^5 for *in vitro* observations. Subsequently, 4 mL α-MEM/10% fetal bovine serum complete culture medium and 10 μL PRP were added to each flask except for three, which were seeded with BMSCs only and α-MEM/10% fetal bovine serum. The culture medium and PRP were renewed every 2 days. Neurogenesis and immunofluorescence were assessed on days 7 and 21 (Figure 1).

Surgical grafting procedures and tissue retrieval

Spinal cord hemi-sectioned female Sprague-Dawley rats (weight, 210–268 g, n = 102) were used. The animals were operated on according to the standard guidelines approved by the Zhejiang University Ethics Committee. The rats were divided into six groups; the numbers of animals used for each group and each examination are listed in Table I. All surgery was performed under sodium pentobarbital anesthesia (40 mg/kg administered intraperitoneally) and sterile conditions. The back musculature was split at the midline, and a laminectomy was performed at T10. After the dura was opened, a spinal cord hemi-section was made with a sharp scalpel as described previously (24); the scalpel was run through the incision to ensure that the hemi-section was complete. The scaffold was placed into the lesion site, and the muscles and skin were sutured (Figure 2D). No active motion of the hind limbs on the injured side was observed in any of the animals after the hemi-section. Rats received cyclosporine and manual bladder expression daily until reflexive bladder control returned. All animals survived the experiment and were used for subsequent analysis; No evidence of tumor or bone formation was observed in any of the animals in our experiment.

Deep anesthesia was administered to 42 rats at 1, 4 and 8 weeks after surgery, and fresh spinal cord containing the injury sites (10 mm in length) was harvested immediately for protein and messenger RNA (mRNA) measurements. Another 60 rats were anesthetized and perfused transcardially with 4% paraformaldehyde in 0.1 mol/L phosphate buffer solution (pH 7.4) at 1, 4 and 8 weeks postoperatively. Spinal cord segments (10 mm in length) were dissected and placed into a 0.1 mol/L phosphate buffer solution containing 30% sucrose for 48 h at 4°C for frozen sections, or post-fixed in the same fixative overnight and embedded in paraffin. Six samples that grafted cells were labeled and were observed using the Maestro In-Vivo Imaging System (CRi, Inc, Woburn, MA, USA). Samples were frozen sectioned in the coronal direction at a 10-μm thickness, then slides were mounted in glycerol/PBS (9:1) containing Hoechst 33258 (2.5 mg/mL; Sigma-Aldrich) to identify the cell nuclei for confocal laser scanning microscopy (CLSM, TCS SP5; Leica, Wetzlar, Germany) observations.

Quantitative reverse transcriptase PCR

Total RNA was isolated using TRIzol Reagent (Invitrogen, Carlsbad, California, USA) in accordance with

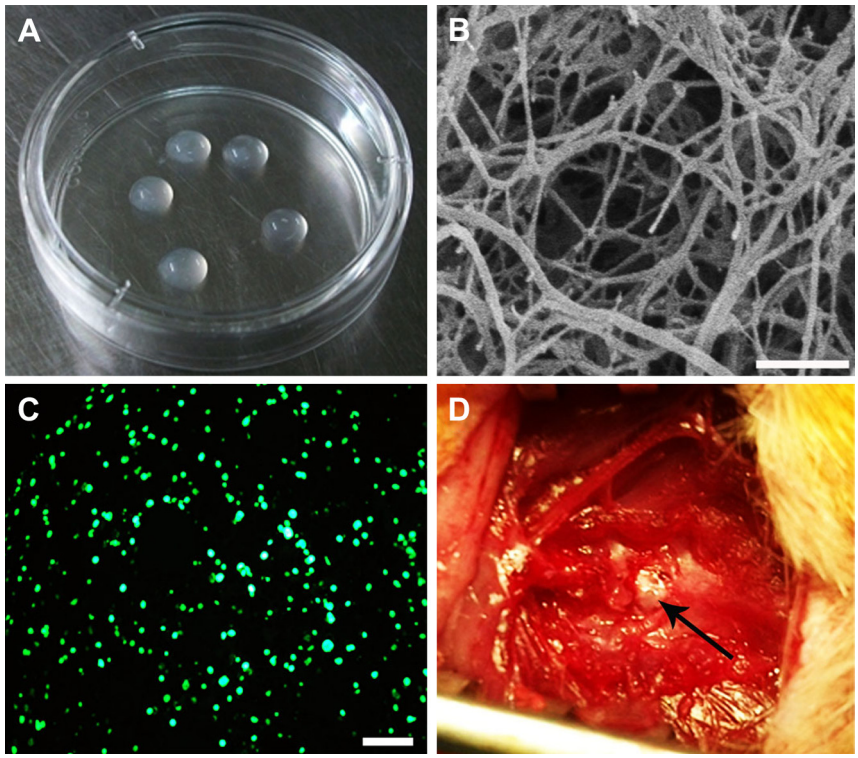

Figure 2. Characteristics of the scaffold and the process of the animal experiment. (A) Prepared scaffolds were transferred to a 35-mm Petri dish and incubated for at least 4 h at 37°C, relative humidity 95% and 5% carbon dioxide. (B) Surface of PRP scaffolds observed with a field emission scanning electron microscope. (C) Image of a 10-μm thick frozen section of the transplant in PRP/BDNF-BMSCs group under a fluorescence microscope. BDNF-BMSCs (green) were scattered in the PRP scaffold. (D) Implantation of scaffolds into the hemisected area (arrows). (Scale bars = 0.4 μm, B, 100 μm, C.)

the manufacturer's instructions. RNA concentrations were determined with a SmartSpec Plus spectrophotometer (Bio-Rad, Tokyo, Japan). Reverse transcription was performed with SuperScript II RTase (Invitrogen), as outlined in the instruction manual. Each group involved four wells. Real-time PCR quantification was performed with SYBR Premix Ex Taq Kit (TaKaRa Bio, Ohtsu, Japan) on an iQTM5 multiplex real-time fluorescence quantitative PCR instrument (Bio-Rad, Bio-Rad, Hercules, CA, USA). The primer sequences specific for the target gene and the internal control gene used for quantitative reverse transcriptase PCR are listed in Table II. β-actin was used as an internal control to adjust the differences between samples. Thermal cycle conditions were 1 min at 95°C for activation of the Universal mixture AmpliTaq Gold Polymerase (Applied Biosystems, Foster City, CA, USA), followed by 45 cycles of 10 s at 95°C for denaturing and 25 s at 62°C for annealing and extension.

Western blot

Spinal cord tissue samples were homogenized in RIPA buffer supplemented with protease inhibitor cocktail and phosphatase inhibitor cocktail (Sigma-Aldrich) for 30 min at 4°C, and the homogenates were centrifuged at 12,000*g* for 15 min at 4°C.

Table II. Nucleotide primers used for quantitative reverse transcriptase PCR.

Genes	Oligonucleotide sequence (5′–3′)	Product size (bp)
NF-200	Forward: GAGGCACTGAAAAGCACCA Reverse: CAAAGCCAATCCGACACTCT	250
GFAP	Forward: AGAAAACCGCATCACCATTC Reverse: GCACACCTCACATCACATCC	188
MAP2	Forward: GGAATAACCAAGAGCCCAGAA Reverse: TCCAGGGGTAGTAGGTGTTGA	201
p70S6K	Forward: TGGCAGGAGTGTTTGACATAG Reverse: CTTTCCATAGCCCCCTTTACC	242
β-actin	Forward: CACCCGCGAGTACAACCTTC Reverse: CCCATACCCACCATCACACC	207

The supernatants were collected, and protein concentrations were determined by the Bradford method using a spectrophotometer. Each sample was separated by 8% SDS-PAGE and blotted. The membrane was incubated with anti-BDNF rabbit polyclonal antibody (AB1534, 1:1000; Chemicon, Temecula, California, USA) and anti-glial fibrillary acidic protein (GFAP) (EPR1034Y, 1:1000; Epitomics, Burlingame, California, USA) overnight at 4°C. Membranes were incubated in Tris-PBS with anti-rabbit IgG conjugated with HRP (1:2000) (Zhongshan Golden Bridge, Beijing, China). Signals were detected on Hyperfilm enhanced chemiluminescence with an imaging system (ChemiDOC XRS, Molecular Imager; BioRad).

Immunofluorescence and immunochemistry

After cells were co-cultured with PRP for days 7 and 21, they were fixed with 70% ethanol and incubated with 100 μL of primary antibody diluted 1:50 in PBS for 1 h at room temperature in the dark. A secondary fluorescence-coupled antibody (Alexa Fluor 555; Molecular Probes) diluted 1:500 was followed for 20 min at room temperature. Three washing steps with PBS and staining were performed thereafter. The neurofilament (NF)-200, GFAP and microtubule-associated protein 2 (MAP2) antibodies (Epitomics) were applied according to published protocols. Cells were examined using the CLSM, and pictures were obtained.

Immunohistochemical procedures were performed as described previously (25). Briefly, serial 5-μm coronal sections around the injured site were mounted on slides and washed three times in PBS, permeabilized with 0.3% Triton X-100 for 5 min and incubated for 1 h with 10% normal goat serum in PBS. The sections were incubated with anti-GFAP rabbit monoclonal antibody (1:100; Epitomics) overnight in 5% normal goat serum in PBS at 4°C. The following day, the sections incubated with secondary antibodies and visualized with diaminobenzidine (PV6001; Zhongshan Golden Bridge). The sections were counterstained with hematoxylin and placed in a coverslip with DPX mountant (Merck, Poole, UK). Some reactions omitted either the primary or the secondary antibody to control for nonspecific background binding.

Ultrastructural studies

For transmission electron microscopy (TEM), specimens were fixed in 1% osmium tetroxide for 2 h and then dehydrated with a serial gradient of ethanol (50%, 70%, 80%, 95%) for 15 min each and then with 100% ethanol for 20 min; the ethanol was changed three times. The blocks were immersed for 5 min in propylene oxide, which was changed twice, and then immersed overnight in a mixture containing equal amounts of propylene oxide and plastic resin and embedded in Epon 812 (EMS, Fort Washington, Pennsylvania, USA). Using TEM, ultra-thin sections (50 nm) were taken with an ultra-microtome, mounted on 150-mesh copper grids and stained with 5% uranyl acetate for 15 min and then with 1.5% lead citrate for 5 min. The sections were examined under an electron microscope (JEM 1230; Jeol Co, Tokyo, Japan). The surface of PRP scaffolds was studied by field emission scanning electron microscopy (S-4800; Hitachi, Ibaraki, Japan).

Quantification of astrocyte migration

For quantification of GFAP-positive astrocytes, three GFAP-stained coronal sections equidistant through the lesion area were used for analysis, using the Image-Pro plus 6.0 (Media Cybernetics, Silver Spring, MD, USA). GFAP immunoreactivity was used as a marker to outline the interface between the grafted and host tissues. We defined the host-graft interface as a starting point "0" to measure the distances of astrocytes that migrated into the lesion area at 200-μm intervals. The number of GFAP-labeled astrocytes is presented as astrocyte index at 0.2-mm, 0.4-mm, 0.6-mm, 0.8-mm, 1.0-mm and 1.2-mm position. Astrocyte index is a ratio of GFAP astrocyte amount at a specific position over the astrocyte amount at "0" position, similar to a recent study (26).

Behavioral testing and statistical analysis

Hind limb motor function was assessed using the open-field Basso-Beattie-Bresnahan (BBB) locomotor rating scale system. Individual rats were placed on an open field and observed for 4 min by two independent blinded examiners. Hind limb function was scored from 0−21 (flaccid paralysis to normal gait). The test was performed 1, 7, 14, 21, 28 and 56 days postoperatively.

Data are presented as mean ± SD. The statistical analysis was performed with an independent sample *t* test to compare two experimental groups and Tukey test for multiple comparisons using SPSS computer software for Windows, version 13.0 (SPSS, Inc, Chicago, Illinois, USA). The level of significance was set at $P < 0.05$.

Results

In vitro

Flow cytometry results revealed that BMSCs expressed CD44, CD73, CD90 and CD105 but not

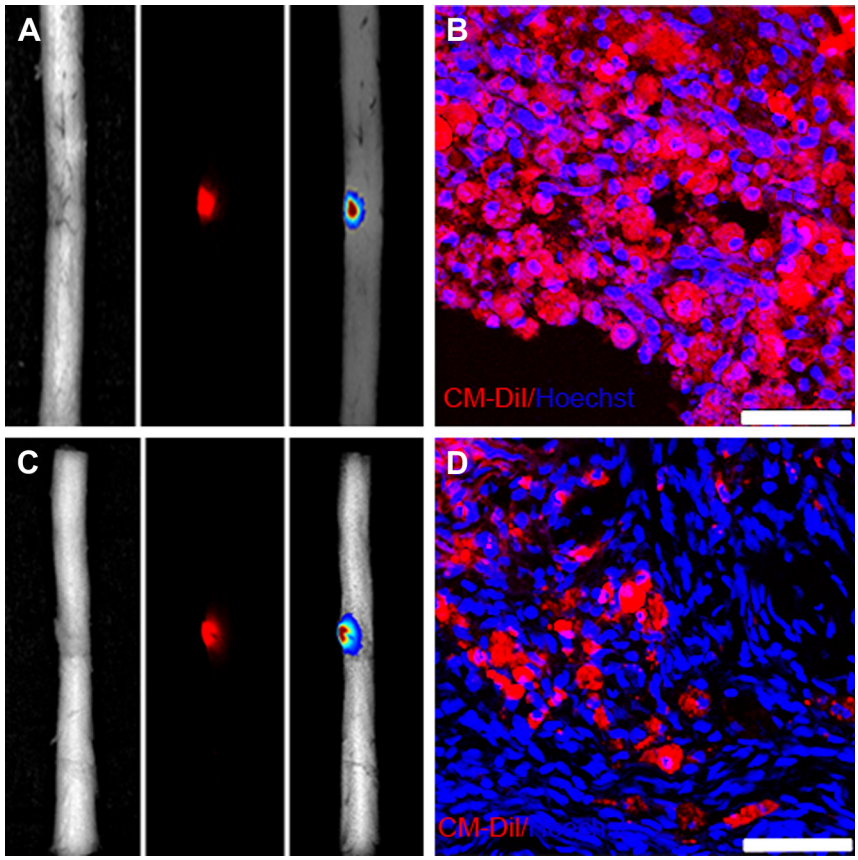

Figure 3. Tracking of rat BMSCs with PRP *in vivo*. Fluorescence images obtained by small animal *in vivo* fluorescence imaging system (A and C) and confocal microscopy after frozen sectioning (B and D). Images A and B and C and D are samples transplanted in PRP/BMSCs group for 1 week and 8 weeks, respectively. Transplanted BMSCs labeled with CM-DiI were identified by cytoplasmic localization of CM-DiI (red) in the injured spinal cord site. At 1 week, the transplanted BMSCs and PRP were mostly confined to the injury area (A and B). At 8 weeks, numerous BMSCs were found outside of the lesion (C and D). (Scale bar = 75 μm, B and D.)

CD45 (see supplementary Figure 1). Of BDNF-BMSCs, 98.49% exhibited green fluorescent protein (GFP) fluorescence. The detection GFP in the BDNF-transduced BMSCs indicates that these cells also expressed rat BDNF because BDNF and GFP were both translated from the same mRNA (Figure 1A). The concentration of BDNF in the supernatant reached 20.36 ± 0.9 ng/10^6 cells/24 h, whereas the amounts of BDNF in the BMSCs and PRP/BMSCs groups were 3.1 ± 0.7 ng/10^6 cells/24 h and 5.1 ± 2.7 ng/10^6 cells/24 h, respectively. The Western blot results also indicated a 3-fold increased expression of BDNF in the engineered BMSCs (Figure 1B).

Expression of NF-200, GFAP, MAP2 and ribosomal protein S6 kinase (p70S6K) genes was analyzed by quantitative reverse transcriptase PCR (Figure 1C–F). These mRNA genes increased in the PRP/BMSCs and PRP/BDNF-BMSCs groups compared with the BMSCs group, especially genes of NF-200, GFAP and MAP2. However, there is no significant expression of NF-200, GFAP and MAP2 by immunofluorescence even at 21 days after culturing with PRP (Figure 1G).

In vivo

The transplanted CM-DiI-labeled BMSCs were easily identified within the lesion zone by their red fluorescence at both 1 week and 8 weeks after transplantation. The distribution of BMSCs in the injured SCI at 1 week and 8 weeks is shown in Figure 3. At 1 week, the transplanted BMSCs and PRP were mostly confined to the injury area (Figure 3A,B). At 8 weeks, numerous BMSCs were found outside of the lesion (Figure 3C,D).

At 7 days postoperatively, we observed an obvious increase in BDNF expression in the injured spinal cords of transplanted BDNF-BMSCs and PRP/BDNF-BMSCs groups by Western blot, indicating that the transplanted BDNF-BMSCs expressed BDNF *in vivo* (Figure 4A). We found a significant increase in BDNF gene expression at 4 weeks post-operatively compared with the other group. A

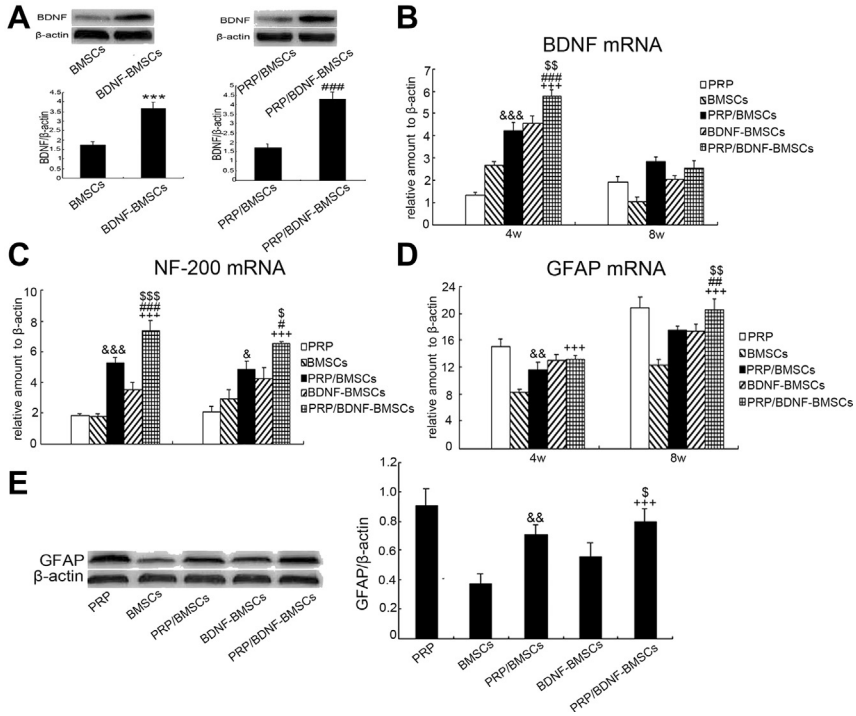

Figure 4. Changes in gene and protein expression after treatment. Western blot results of BDNF in BDNF-BMSCs and PRP/BDNF-BMSCs groups at 7 days after SCI (A). Gene expression of BDNF in all groups at 4 weeks and 8 weeks (B). GFAP and NF-200 mRNA increased in the PRP/BDNF-BMSCs group at 4 weeks and 8 weeks postoperatively (C and D). $^{***}P < 0.001$ (BDNF-BMSCs vs. BMSCs), $^{\$}$ or $^{\$\$}$ or $^{\$\$\$}P < 0.05$ or $P < 0.01$ or $P < 0.001$ (PRP/BDNF-BMSCs vs. BDNF-BMSCs), $^{\#}$ or $^{\#\#}$ or $^{\#\#\#}P < 0.05$ or $P < 0.01$ or $P < 0.001$ (PRP/BDNF-BMSCs vs. PRP/BMSCs), $^{+++}P < 0.001$ (PRP/BDNF-BMSCs vs. BMSCs alone), $^{\&\&}$ or $^{\&\&\&}P < 0.01$ or $P < 0.001$ (PRP/BMSCs vs. BMSCs alone).

significant increase in NF-200 mRNA was detected after applying PRP with BMSCs or engineered BMSCs (Figure 4C), and the PRP/BDNF-BMSCs group expressed more NF-200 than other groups at 4 weeks and 8 weeks postoperatively. All PRP groups (PRP, PRP/BMSCs and PRP/BDNF-BMSCs) showed increased GFAP expression both at the gene and at the protein levels compared with control groups (BMSCs and BDNF-BMSCs) at 8 weeks (Figure 4D,E), although there were no significant differences between PRP/BDNF-BMSCs and BDNF-BMSCs groups at 4 weeks postoperatively (Figure 4D).

Histologic examination performed 8 weeks after hemi-sectioning the spinal cord revealed that few astrocytes were observed in the epicenter of the injury in the vehicle-treated group, and a cyst cavity had formed in the PRP group (Figure 5A,B). In the BMSCs group, GFAP-positive cells had a disorderly arrangement, and there were numerous small, round lymphocytes diffused in the injured spinal cord (Figure 5C). All PRP groups showed significantly more astrocytes in the lesion site compared with control groups ($P < 0.05$). Few astrocytes migrated into the graft region in the vehicle-treated and PRP groups; most astrocytes were observed in the interface of the cavity. A modest number of astrocytes migrated into the lesion center in the BMSCs group. In contrast, in grafts when PRP was co-transplanted with BMSCs or only BDNF overexpressing BMSCs, more migration of astrocytes into the transplants was observed (Figure 5D,E). In the PRP/BDNF-BMSCs group, astrocytes migrated throughout the entire length of the lesion area, as they were seen in the rostral and caudal graft segments by immunohistochemistry (Figure 5F,G). The astrogliotic response at the graft-host interface of BDNF-BMSCs and PRP/BDNF-BMSCs groups was reduced compared with the vehicle-treated and PRP groups (Figure 5H). In the PRP/BMSCs group, 40% more GFAP-positive astrocytes were found at the graft-host interface than in the PRP/BDNF-BMSCs group ($P = 0.003$), whereas there were no significant differences among the vehicle-treated, BDNF-BMSCs and PRP/BDNF-BMSCs groups.

TEM revealed severe demyelination in the vehicle-treated, PRP and BMSCs groups. Hollow and collapse of sheaths emerged in the vehicle-treated group (Figure 6A). The PRP and BMSCs groups showed detached and disrupted myelin sheets on the myelinated axons (Figure 6B,C). There were also whirled body and vacuole formations in the myelinated axons, especially in the BMSCs group. In

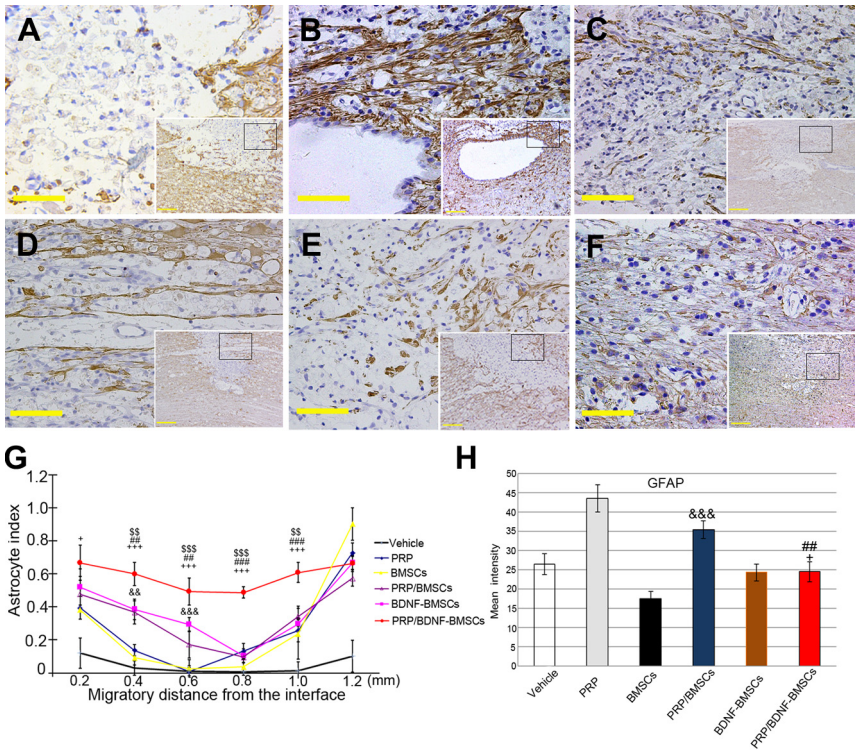

Figure 5. Histologic analysis of the astrocyte process and astrogliotic response. (A–F) Immunostaining with the anti-GFAP antibody in sections of the vehicle-treated group at week 8 after SCI (A), PRP group (B), rat BMSCs group (C), PRP/BMSCs group (D), BDNF-BMSCs group (E) and PRP/BDNF-BMSCs group (F). (Scale bars = 50 μm, A, B, C, D, E, F; 250 μm, inset of A, B, C, D, E, F.) (G) Statistical analysis of the astrocyte process in the lesion zone of experiment groups. (H) Astrogliotic response at the graft-host interface of the experimental groups. n = 15, $^{\$\$}$ or $^{\$\$\$}P < 0.01$ or $P < 0.001$ (PRP/BDNF-BMSCs vs. BDNF-BMSCs), $^{\#\#}$ or $^{\#\#\#}P < 0.01$ or $P < 0.001$ (PRP/BDNF-BMSCs vs. PRP/BMSCs), $^{+}$ or $^{+++}P < 0.05$ or $P < 0.001$ (PRP/BDNF-BMSCs vs. BMSCs alone), $^{\&\&}$ or $^{\&\&\&}P < 0.01$ or $P < 0.001$ (PRP/BMSCs vs. BMSCs alone).

contrast, the disruption of myelin sheets in the PRP/BMSCs group was mild (Figure 6D). Demyelination in the BDNF-BMSCs group was partially inhibited, with more myelin sheaths spared (Figure 6E). However, there was significant axonal remyelination and the more active oligodendrocytes in the PRP/BDNF-BMSCs group at 8 weeks (Figure 6F).

Motor function of the right leg was intact, and 21 points were scored for all animals before SCI. All experimental animals exhibited a gradual improvement in hind limb locomotor function during the 8-week recovery period. The PRP/BDNF-BMSCs group recovered with a BBB score (Basso-Beattie-Bresnahan locomotor rating scale system) of nearly 20 (Figure 7). Statistical analyses indicated that the BBB scores of the PRP/BDNF-BMSCs group were higher than the BBB scores in other groups at 8 weeks after transplantation ($P < 0.05$).

Discussion

The present study demonstrated that a combination of PRP scaffolds with BDNF-overexpressing BMSCs had a synergistic effect on promoting astrocyte migration and axonal remyelination. The results revealed a beneficial effect of PRP scaffold and BMSCs locally applied into the injury area of the spinal cord, which was similar to the effect of BDNF-BMSCs transplantation alone. These results were in accordance with previous studies. Hiraizumi *et al.* (27) used platelet-derived wound healing formula to improve the extracellular microenvironment of the remaining neurons, and Sasaki *et al.* (19) demonstrated that BDNF-modified human BMSCs had additive neuroprotective effects and increased axonal sprouting.

In our *in vitro* study, we investigated gene changes after the BMSCs or BDNF-BMSCs co-cultured with PRP for 7 days and 21 days. The increased expression of the NF-200, GFAP and MAP2 genes indicated that PRP promoted BMSCs expression of neuronal gene markers in gene levels. In the PRP/BDNF-BMSCs group, the expression of these genes was higher than in the other groups, indicating PRP and BDNF have additive effects on BMSCs compared with using PRP or BDNF alone, as described previously (21). p70S6K, a downstream target of phosphoinositide 3-kinase (PI3K)/mammalian target of rapamycin (mTOR) signaling, is a mediator of protein translation and cell growth

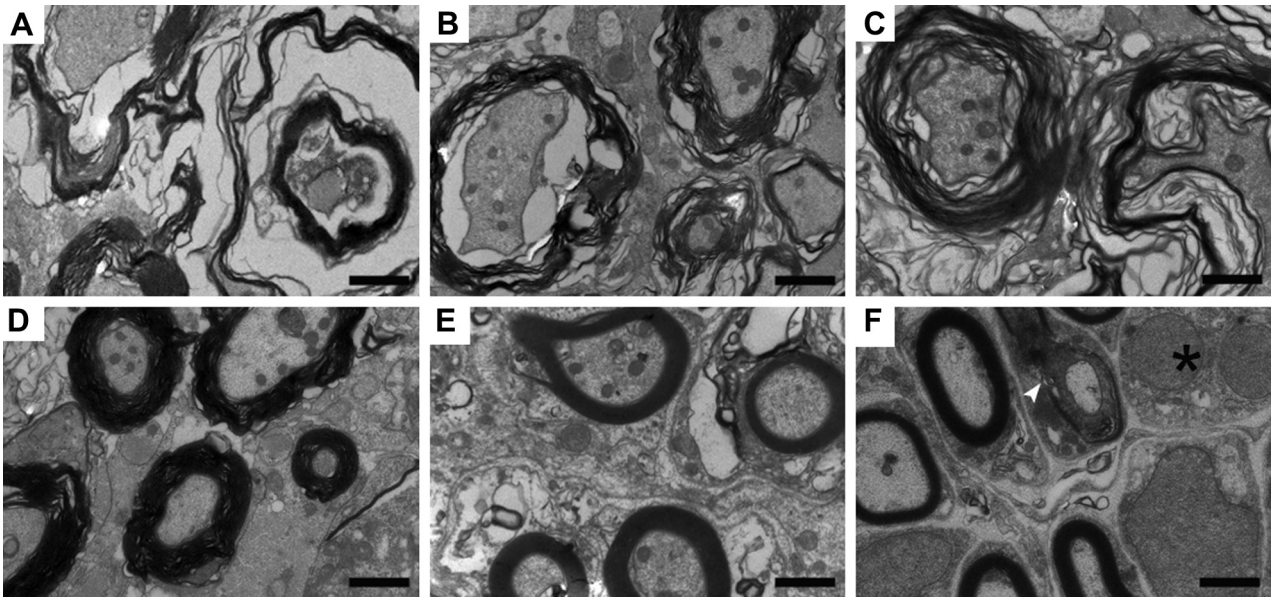

Figure 6. Transmission electron microphotographs show myelin changes after SCI at 8 weeks after surgery. (A) In the vehicle-treated group, hollow and collapse of sheaths emerged. (B and C) Demyelination with detachment and disruption of myelin sheets and formation of whirled bodies and vacuoles in the myelinated axons in PRP and BMSCs groups. Severe demyelination and axonal degeneration in BMSCs group. (D) Mild disruption of myelin sheets in PRP/BMSCs group. (E) Demyelination in BDNF-BMSCs group was inhibited partly, with more myelin sheaths remaining. (F) In PRP/BDNF-BMSCs group, formation of myelin sheets (white arrow) and the more active oligodendrocytes (asterisk). (Scale bar = 1 μm.)

(28). The mRNA of p70S6K in the PRP/BMSCs and PRP/BDNF-BMSCs groups was promoted at 7 days and 21 days, suggesting that PRP stimulated cell growth in these groups (29). The virus might decrease the BMSCs proliferation more or less (30), as more genes of p70S6K were detected in PRP/BMSCs than PRP/BDNF-BMSCs group. We cultured BMSCs with PRP in liquid form and renewed the PRP every other day. Some experiments suggested that culturing BMSCs in PRP without thrombin might be a better choice for expanding BMSCs *in vivo* for clinical use (31). However, the significant expression of NF-200, GFAP and MAP2 by immunofluorescence was not detected after co-culturing for 7 days and 21 days. The reason might be that BMSCs in the monolayer culture with PRP do not have neuronal potential, whereas BMSCs cultured in a three-dimensional environment might possess the ability (32–34).

The implantation of 15-μL scaffolds separated the terminal of the transected spinal cord completely (with a distance of 1.2 mm); however, this created a tight junction in the injured terminals by clot retraction at the same time. The hemi-section model allows for precise, consistent and reproducible severing of the spinal cord. It is an injury similar to that caused by stab wounds, gunshots and other penetrating injuries to the spinal cord (35).

BDNF levels assayed by Western blot in the hemi-sected spinal cord increased at 7 days postoperatively in all PRP groups, but the level was significantly higher in the PRP/BDNF-BMSCs group. Previous studies showed that BMSCs could secret BDNF (29,36), which was consistent with the BMSCs group of this study. Expression of BDNF and NF-200 was up-regulated in the PRP/BDNF-BMSCs group at 4 weeks postoperatively; this indicates that the BDNF-BMSCs could maintain high levels of BDNF during the post-injury period and trigger the up-regulation of NF-200 mRNA in the spinal cord (37). An additional trophic effect is needed to promote axonal regeneration and the expression of neurofilament after SCI (38,39).

Accumulations of astrocytes, which participate in the formation of the glial scar at the interface of the injury area, were an inhibitory barrier for neural regeneration (40). Some more recent studies have suggested that astrocytes may protect neurons after injury (41). As we revealed that PRP inducing astrocytic cell fate is weak *in vitro*, and a previous study suggested BDNF-BMSCs did not differentiate into glial or neuronal elements *in vivo* (19,42), the astrocytes emerging in the epicenter of injury of the present study were considered as migration of host astrocytes. Treatment with only PRP promotes astrocyte proliferation but with little migration, leading to the formation of glial scar at the interface of the cyst cavity. The transplantation of PRP and BMSCs decreased the accumulation of astrocytes,

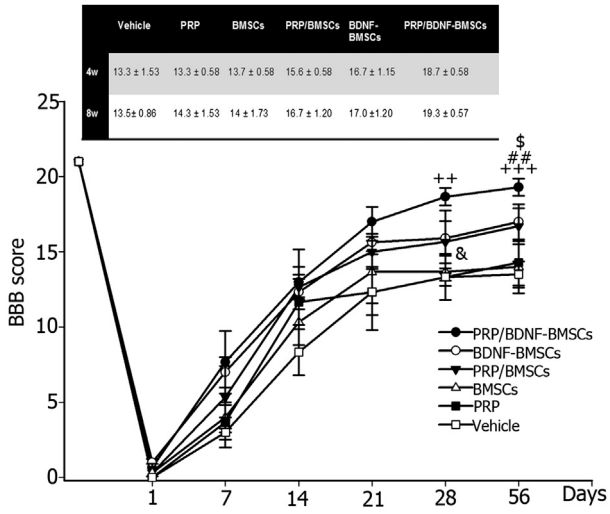

Figure 7. Behavioral analysis of locomotor function. Open-field locomotor scores for PRP/BDNF-BMSCs, BDNF-BMSCs, PRP/BMSCs, BMSCs and PRP groups (n = 8/group) tested at 1, 7, 14, 21, 28 and 56 days after transplantation. The PRP/BDNF-BMSCs transplant group recovered to nearly 20 on the BBB scale. A statistical analysis indicated that the BBB scores at 4 weeks and 8 weeks after injury in the PRP/BDNF-BMSCs transplantation group were significantly higher than the BBB scores of the PRP/BMSCs, BMSCs, PRP and vehicle-treated groups. $^{\$}P < 0.05$ (PRP/BDNF-BMSCs vs. BDNF-BMSCs), $^{\#\#}P < 0.01$ (PRP/BDNF-BMSCs vs. PRP/BMSCs), $^{++}$ or $^{+++}P < 0.01$ or $P < 0.001$ (PRP/BDNF-BMSCs vs. BMSCs alone), $^{\&}P < 0.05$ (PRP/BMSCs vs. BMSCs alone).

and robust astrocytes migrated into the epicenter of the injury. However, major migration of astrocytes was also observed in the BDNF-BMSCs group; BDNF was suggested to induce a premature transformation of glia into astrocytes by increasing bone morphogenetic protein-7 expression (43). The expression of GFAP was the highest in the PRP/BDNF-BMSCs group compared with other groups (except the PRP group) at 8 weeks after surgery. In addition, there were fewer astrocytes at the graft-host interface; this might be explained by the fact that most migration of astrocytes occurred into the graft environment in the PRP/BDNF-BMSCs group (Figure 5).

The astrocyte-oligodendrocyte/myelin interaction was believed to play an important role in the remyelination process (44,45), although the increased expression of BDNF promotes remyelination of axons by affecting oligodendrocytes (46,47). We could find more spared axonal remyelination and oligodendrocytes in PRP/BDNF-BMSCs group by ultrastructural examination; this may be attributed to the increased migration of astrocytes into the lesion area and grafted BDNF-BMSCs, which can provide a favorable substrate for stabilizing the regenerating axons in the inhibitory environment (48,49). The PRP/BDNF-BMSCs group showed a better functional result, which followed a greater amount of axonal remyelination.

There are several limitations to this study. First, CM-DiI was used to track the transplanted BMSCs to confirm the transplanted BMSCs were alive during the 8-week period. However, DiI was reported to be represented by phagocytic cells followed by donor cell apoptosis, and BMSCs outside of the lesion may be due to the movement of macrophage (50), making it difficult to determine the fate of the transplanted cells. Although it was reported that BMSCs transduced with the adenoviral vectors produced greater target gene expression compared with BMSCs transduced with lentiviral vector (51), the decreased expression of target gene after 4 weeks *in vivo* makes it difficult to observe the expression of GFP (52). Our future research will focus on culturing BMSCs in three-dimensional growth systems (with or without PRP) and involve a new strategy to elaborate the mechanism of BMSCs migration after delivery. Second, the concentrations of key growth factors in PRP that were involved in axonal growth, differentiation of BMSCs and synthesis of matrix components were not measured in the present study. A controversial factor with the application of PRP is different methods of its preparation because it can significantly influence the concentration of platelets and growth factors and consequently their repair capacity (53). More recent research suggested that reduced platelet concentration did not harm PRP effectiveness for tissue repairs *in vivo* (54).

In conclusion, despite such limitations, we believe that this study provides valuable information on the influence of a PRP scaffold in the treatment of SCI. Transplantation of autologous BMSCs or programmed BMSCs in conjunction with a PRP scaffold might provide therapeutic opportunities for improving axonal remyelination and functional recovery in humans.

Acknowledgments

This research is financially supported by the National Natural Science Foundation of China (Grant No. 81171703, 81101377, 81171687, and 81271356), the Natural Science Foundation of Zhejiang, China (Grant No. Y207216, Y2100161, Y2090283), the Scientific Research Fund of Zhejiang Provincial Education Department (Y201018936) and the key project of Zhejiang Provincial Department of science and technology (2011C13033).

Disclosure of interest: The authors have no commercial, proprietary, or financial interest in the products or companies described in this article.

References

1. Harel NY, Strittmatter SM. Can regenerating axons recapitulate developmental guidance during recovery from spinal cord injury? Nat Rev Neurosci. 2006;7:603–16.
2. Parikh P, Hao Y, Hosseinkhani M, Patil SB, Huntley GW, Tessier-Lavigne M, et al. PNAS Plus. Regeneration of axons in injured spinal cord by activation of bone morphogenetic protein/Smad1 signaling pathway in adult neurons. Proc Natl Acad Sci U S A. 2011;108:E99–107.
3. Jain A, McKeon RJ, Brady-Kalnay SM, Bellamkonda RV. Sustained delivery of activated Rho GTPases and BDNF promotes axon growth in CSPG-rich regions following spinal cord injury. PLoS One. 2011;6:e16135.
4. Satake K, Lou J, Lenke LG. Migration of mesenchymal stem cells through cerebrospinal fluid into injured spinal cord tissue. Spine (Phila Pa 1976). 2004;29:1971–9.
5. Menei P, Montero-Menei C, Whittemore SR, Bunge RP, Bunge MB. Schwann cells genetically modified to secrete human BDNF promote enhanced axonal regrowth across transected adult rat spinal cord. Eur J Neurosci. 1998;10:607–21.
6. Grill R, Murai K, Blesch A, Gage FH, Tuszynski MH. Cellular delivery of neurotrophin-3 promotes corticospinal axonal growth and partial functional recovery after spinal cord injury. J Neurosci. 1997;17:5560–72.
7. Ruitenberg MJ, Plant GW, Christensen CL, Blits B, Niclou SP, Harvey AR, et al. Viral vector-mediated gene expression in olfactory ensheathing glia implants in the lesioned rat spinal cord. Gene Ther. 2002;9:135–46.
8. Qi Y, Zhao T, Yan W, Xu K, Shi Z, Wang J. Mesenchymal stem cell sheet transplantation combined with locally released simvastatin enhances bone formation in a rat tibia osteotomy model. Cytotherapy. 2013;15:44–56.
9. Samadikuchaksaraei A. An overview of tissue engineering approaches for management of spinal cord injuries. J Neuroeng Rehabil. 2007;4:15.
10. Egawa-Tsuzuki T, Ohno M, Tanaka N, Takeuchi Y, Uramoto H, Faigle R, et al. The PDGF B-chain is involved in the ontogenic susceptibility of the developing rat brain to NMDA toxicity. Exp Neurol. 2004;186:89–98.
11. McTigue DM, Popovich PG, Morgan TE, Stokes BT. Localization of transforming growth factor-beta1 and receptor mRNA after experimental spinal cord injury. Exp Neurol. 2000;163:220–30.
12. Ozdinler PH, Macklis JD. IGF-I specifically enhances axon outgrowth of corticospinal motor neurons. Nat Neurosci. 2006;9:1371–81.
13. Ding XG, Li SW, Zheng XM, Hu LQ, Hu WL, Luo Y. The effect of platelet-rich plasma on cavernous nerve regeneration in a rat model. Asian J Androl. 2009;11:215–21.
14. Emel E, Ergun SS, Kotan D, Gursoy EB, Parman Y, Zengin A, et al. Effects of insulin-like growth factor-I and platelet-rich plasma on sciatic nerve crush injury in a rat model. J Neurosurg. 2011;114:522–8.
15. Farrag TY, Lehar M, Verhaegen P, Carson KA, Byrne PJ. Effect of platelet rich plasma and fibrin sealant on facial nerve regeneration in a rat model. Laryngoscope. 2007;117:157–65.
16. Cho HH, Jang S, Lee SC, Jeong HS, Park JS, Han JY, et al. Effect of neural-induced mesenchymal stem cells and platelet-rich plasma on facial nerve regeneration in an acute nerve injury model. Laryngoscope. 2010;120:907–13.
17. Sariguney Y, Yavuzer R, Elmas C, Yenicesu I, Bolay H, Atabay K. Effect of platelet-rich plasma on peripheral nerve regeneration. J Reconstr Microsurg. 2008;24:159–67.
18. Zhou L, Shine HD. Neurotrophic factors expressed in both cortex and spinal cord induce axonal plasticity after spinal cord injury. J Neurosci Res. 2003;74:221–6.
19. Sasaki M, Radtke C, Tan AM, Zhao P, Hamada H, Houkin K, et al. BDNF-hypersecreting human mesenchymal stem cells promote functional recovery, axonal sprouting, and protection of corticospinal neurons after spinal cord injury. J Neurosci. 2009;29:14932–41.
20. Hiebert GW, Khodarahmi K, McGraw J, Steeves JD, Tetzlaff W. Brain-derived neurotrophic factor applied to the motor cortex promotes sprouting of corticospinal fibers but not regeneration into a peripheral nerve transplant. J Neurosci Res. 2002;69:160–8.
21. Zurita M, Otero L, Aguayo C, Bonilla C, Ferreira E, Parajon A, et al. Cell therapy for spinal cord repair: optimization of biologic scaffolds for survival and neural differentiation of human bone marrow stromal cells. Cytotherapy. 2010;12:522–37.
22. Qi YY, Chen X, Jiang YZ, Cai HX, Wang LL, Song XH, et al. Local delivery of autologous platelet in collagen matrix simulated in situ articular cartilage repair. Cell Transplant. 2009;18:1161–9.
23. Cao L, Su Z, Zhou Q, Lv B, Liu X, Jiao L, et al. Glial cell line-derived neurotrophic factor promotes olfactory ensheathing cells migration. Glia. 2006;54:536–44.
24. King VR, Hewazy D, Alovskaya A, Phillips JB, Brown RA, Priestley JV. The neuroprotective effects of fibronectin mats and fibronectin peptides following spinal cord injury in the rat. Neuroscience. 2010;168:523–30.
25. Xu K, Uchida K, Nakajima H, Kobayashi S, Baba H. Targeted retrograde transfection of adenovirus vector carrying brain-derived neurotrophic factor gene prevents loss of mouse (twy/twy) anterior horn neurons in vivo sustaining mechanical compression. Spine (Phila Pa 1976). 2006;31:1867–74.
26. Deng LX, Hu J, Liu N, Wang X, Smith GM, Wen X, et al. GDNF modifies reactive astrogliosis allowing robust axonal regeneration through Schwann cell-seeded guidance channels after spinal cord injury. Exp Neurol. 2011;229:238–50.
27. Hiraizumi Y, Fujimaki E, Transfeldt EE, Kawahara N, Fiegel VD, Knighton D, et al. The effect of the platelet derived wound healing formula and the nerve growth factor on the experimentally injured spinal cord. Spinal Cord. 1996; 34:394–402.
28. Liu K, Lu Y, Lee JK, Samara R, Willenberg R, Sears-Kraxberger I, et al. PTEN deletion enhances the regenerative ability of adult corticospinal neurons. Nat Neurosci. 2010;13: 1075–81.
29. van den Dolder J, Mooren R, Vloon AP, Stoelinga PJ, Jansen JA. Platelet-rich plasma: quantification of growth factor levels and the effect on growth and differentiation of rat bone marrow cells. Tissue Eng. 2006;12:3067–73.
30. Thomas CE, Birkett D, Anozie I, Castro MG, Lowenstein PR. Acute direct adenoviral vector cytotoxicity and chronic, but not acute, inflammatory responses correlate with decreased vector-mediated transgene expression in the brain. Mol Ther. 2001;3:36–46.
31. Hu Z, Peel SA, Ho SK, Sandor GK, Clokie CM. Platelet-rich plasma induces mRNA expression of VEGF and PDGF in rat bone marrow stromal cell differentiation. Oral Surg Oral Med Oral Pathol Oral Radiol Endod. 2009;107:43–8.
32. Drengk A, Zapf A, Sturmer EK, Sturmer KM, Frosch KH. Influence of platelet-rich plasma on chondrogenic differentiation and proliferation of chondrocytes and mesenchymal stem cells. Cells Tissues Organs. 2009;189:317–26.
33. Chen WH, Liu HY, Lo WC, Wu SC, Chi CH, Chang HY, et al. Intervertebral disc regeneration in an ex vivo culture system using mesenchymal stem cells and platelet-rich plasma. Biomaterials. 2009;30:5523–33.
34. Huang S, Jia S, Liu G, Fang D, Zhang D. Osteogenic differentiation of muscle satellite cells induced by platelet-rich

plasma encapsulated in three-dimensional alginate scaffold. Oral Surg Oral Med Oral Pathol Oral Radiol. 2012;114: S32–40.
35. Mautes AE, Weinzierl MR, Donovan F, Noble LJ. Vascular events after spinal cord injury: contribution to secondary pathogenesis. Phys Ther. 2000;80:673–87.
36. Xiong Y, Mahmood A, Chopp M. Angiogenesis, neurogenesis and brain recovery of function following injury. Curr Opin Invest Drugs. 2010;11:298–308.
37. Nomura T, Honmou O, Harada K, Houkin K, Hamada H, Kocsis JD. I.V. infusion of brain-derived neurotrophic factor gene-modified human mesenchymal stem cells protects against injury in a cerebral ischemia model in adult rat. Neuroscience. 2005;136:161–9.
38. Busch SA, Hamilton JA, Horn KP, Cuascut FX, Cutrone R, Lehman N, et al. Multipotent adult progenitor cells prevent macrophage-mediated axonal dieback and promote regrowth after spinal cord injury. J Neurosci. 2011;31:944–53.
39. Shen Y, Tenney AP, Busch SA, Horn KP, Cuascut FX, Liu K, et al. PTPsigma is a receptor for chondroitin sulfate proteoglycan, an inhibitor of neural regeneration. Science (New York, NY). 2009;326:592–6.
40. Wanner IB, Deik A, Torres M, Rosendahl A, Neary JT, Lemmon VP, et al. A new in vitro model of the glial scar inhibits axon growth. Glia. 2008;56:1691–709.
41. Barreto G, White RE, Ouyang Y, Xu L, Giffard RG. Astrocytes: targets for neuroprotection in stroke. Cent Nerv Syst Agents Med Chem. 2011;11:164–73.
42. Lu P, Jones LL, Tuszynski MH. BDNF-expressing marrow stromal cells support extensive axonal growth at sites of spinal cord injury. Exp Neurol. 2005;191:344–60.
43. Ortega JA, Alcantara S. BDNF/MAPK/ERK-induced BMP7 expression in the developing cerebral cortex induces premature radial glia differentiation and impairs neuronal migration. Cereb Cortex. 2010;20:2132–44.
44. Smith-Thomas LC, Stevens J, Fok-Seang J, Faissner A, Rogers JH, Fawcett JW. Increased axon regeneration in astrocytes grown in the presence of proteoglycan synthesis inhibitors. J Cell Sci. 1995;108(Pt 3):1307–15.
45. Schulz K, Kroner A, David S. Iron efflux from astrocytes plays a role in remyelination. J Neurosci. 2012;32:4841–7.
46. Lang EM, Schlegel N, Reiners K, Hofmann GO, Sendtner M, Asan E. Single-dose application of CNTF and BDNF improves remyelination of regenerating nerve fibers after C7 ventral root avulsion and replantation. J Neurotrauma. 2008;25:384–400.
47. VonDran MW, Singh H, Honeywell JZ, Dreyfus CF. Levels of BDNF impact oligodendrocyte lineage cells following a cuprizone lesion. J Neurosci. 2011;31:14182–90.
48. Hawthorne AL, Hu H, Kundu B, Steinmetz MP, Wylie CJ, Deneris ES, et al. The unusual response of serotonergic neurons after CNS injury: lack of axonal dieback and enhanced sprouting within the inhibitory environment of the glial scar. J Neurosci. 2011;31:5605–16.
49. Busch SA, Horn KP, Cuascut FX, Hawthorne AL, Bai L, Miller RH, et al. Adult NG2+ cells are permissive to neurite outgrowth and stabilize sensory axons during macrophage-induced axonal dieback after spinal cord injury. J Neurosci. 2010;30:255–65.
50. Horn KP, Hawthorne AL, van Rooijen N, Silver J. Another barrier to regeneration in the CNS: activated macrophages induce extensive retraction of dystrophic axons through direct physical interactions. J Neurosci. 2012;28:9330–41.
51. Virk MS, Conduah A, Park SH, Liu N, Sugiyama O, Cuomo A, et al. Influence of short-term adenoviral vector and prolonged lentiviral vector mediated bone morphogenetic protein-2 expression on the quality of bone repair in a rat femoral defect model. Bone. 2008;42:921–31.
52. Abdellatif AA, Pelt JL, Benton RL, Howard RM, Tsoulfas P, Ping P, et al. Gene delivery to the spinal cord: comparison between lentiviral, adenoviral, and retroviral vector delivery systems. J Neurosci Res. 2006;84:553–67.
53. Duan J, Kuang W, Tan J, Li H, Zhang Y, Hirotaka K, et al. Differential effects of platelet rich plasma and washed platelets on the proliferation of mouse MSC cells. Mol Biol Rep. 2011; 38:2485–90.
54. Mastrangelo AN, Vavken P, Fleming BC, Harrison SL, Murray MM. Reduced platelet concentration does not harm PRP effectiveness for ACL repair in a porcine in vivo model. J Orthop Res. 2011;29:1002–7.

Supplementary data

Supplementary data related to this article can be found online at http://dx.doi.org/10.1016/j.jcyt.2013.04.004